HHS Public Access

Author manuscript

Nat Neurosci. Author manuscript; available in PMC 2012 March 01.

Published in final edited form as:

Nat Neurosci. ; 14(9): 1109–1111. doi:10.1038/nn.2895.

Harmonin inhibits presynaptic $Ca_v1.3$ Ca^{2+} channels in mouse inner hair cells

Frederick D. Gregory[1,2,*], **Keith E. Bryan**[1,*], **Tina Pangršič**[3,*], **Irina E. Calin-Jageman**[2,*,#], **Tobias Moser**[3], and **Amy Lee**[1]

[1]Depts. of Molecular Physiology & Biophysics, Otolaryngology-Head and Neck Surgery, and Neurology, University of Iowa

[2]Depts. of Pharmacology and Physiology, Emory University

[3]InnerEarLab, Dept. of Otolaryngology and Center for Molecular Physiology of the Brain, Bernstein Center for Computational Neuroscience, University of Goettingen

Abstract

Harmonin is a scaffolding protein required for normal mechanosensory function in hair cells. Here, we describe a novel presynaptic association of harmonin and $Ca_v1.3$ Ca^{2+} channels at the mouse inner hair cell synapse, which limits channel availability through a ubiquitin-dependent pathway.

Voltage-gated $Ca_v1.3$ (L-type) Ca^{2+} channels mediate Ca^{2+} influx and exocytosis at the inner hair cell (IHC) synapse and are required for hearing[1,2]. The C-terminus of the $Ca_v1.3$ α_1 subunit ($\alpha_1$1.3) binds to PDZ (PSD-95 (Postsynaptic density-95)/Discs large/ZO-1 (Zona occludens-1) domains, which affect neuronal $Ca_v1.3$ localization and function[3]. In screening for PDZ-proteins that interact with Ca_v1 α_1-subunits, we discovered that harmonin (variant *a*), a PDZ-protein expressed in IHCs[4], binds to $\alpha_1$1.3 via the second of its three PDZ domains (Fig. 1a,b).

Like the PDZ-protein erbin[5], harmonin promoted voltage-dependent facilitation of $Ca_v1.3$ in transfected HEK293T cells (not shown). However, harmonin also significantly suppressed peak $Ca_v1.3$ Ba^{2+} current (I_{Ba}) density (~66%, $p<0.001$; Fig. 1c) without major effects on voltage-dependent activation (Supplementary table 1). Harmonin significantly decreased maximal "on" gating charge (Q_{on}) of I_{Ba} and tail current amplitudes at the reversal potential

Correspondence to: Amy Lee, Dept. of Molecular Physiology and Biophysics, University of Iowa, 5-610 Bowen Science Building, 51 Newton Rd., Iowa City, IA 52242, Phone: (319) 384-1762, FAX: (319) 335-7330, amylee@uiowa.edu.

*Denotes equal contributions

#Present address: Dept. of Biological Sciences, Dominican University

AUTHOR CONTRIBUTIONS:

FDG conducted the patch-clamp recordings of transfected HEK293T cells and mouse inner hair cells; KEB performed the biochemical and immunofluorescence analyses of ubiquitinated channels; TP performed the Ca^{2+} imaging of mouse inner hair cells; IEC performed the biochemical characterizations of harmonin/$Ca_V1.3$ interactions; TM and AL assisted with experimental design, data analysis, and interpretation. All authors contributed to writing of the manuscript.

Declaration of competing financial interests

(Fig. 1d, Supplementary Fig. 1), which suggests that harmonin reduces the number of available $Ca_v1.3$ channels rather than the open probability. Disrupting the type I PDZ binding sequence of $\alpha_1 1.3$ by substituting the C-terminal leucine for alanine (L-A) prevented harmonin binding (Fig. 1e) and inhibition of $Ca_v1.3$ peak current density (p=0.93; Fig. 1f).

As described previously [6-8], harmonin is strongly localized in the apical hair bundles of IHCs (Supplementary Fig.2). However, closer scrutiny revealed harmonin clusters at the base of IHCs, which colocalized with the ribbon synapse protein ribeye/CtBP2 at a subset of synapses (Fig. 1g). Comparisons before (P6–8) and after (P14–16) hearing onset revealed a developmental increase in the number of harmonin-positive IHC synapses (Fig. 1g). In most immature IHCs (30 of 35), harmonin was localized at ~10–30% of synapses per IHC. However, in mature IHCs (18 of 31), ~40–60% of synapses per IHC were harmonin-positive (Fig. 1g). $Ca_v1.3$ channels may be necessary for the synaptic localization of harmonin: the fraction of harmonin-positive synapses was significantly reduced in IHCs from *$Ca_v1.3^{-/-}$* mice (~26% of harmonin-positive synapses in WT, P6-8, n=84 IHCs, vs. ~10% in *$Ca_v1.3^{-/-}$*, P6-8, n=82 IHCs, p<0.001; Fig. 1g). Harmonin also coimmunoprecipitated with $Ca_v1.3$ from cochlear extracts (Supplementary Fig. 2). These findings support a presynaptic association of harmonin with $Ca_v1.3$, primarily in mature IHCs.

To determine if harmonin regulates presynaptic $Ca_v1.3$ channels in IHCs, we analyzed "deaf-circler" mice (*dfcr*)[9]. While the mutant (*dfcr* harmonin) retains PDZ2 that interacts with $\alpha_1 1.3$ (Fig. 1b), an internal deletion removes the coiled-coil domain and causes abnormal proximity of the PDZ domains. *Dfcr* harmonin did not bind to $\alpha_1 1.3$ (Fig. 2a) or affect peak $Ca_v1.3$ I_{Ba} density in transfected HEK293T cells (p=0.10; Fig. 2b), which demonstrates that *dfcr* harmonin does not functionally interact with $\alpha_1 1.3$. In agreement with a normally inhibitory role for harmonin, whole cell I_{Ba} density was greater in P16–18 *dfcr* IHCs than in control IHCs (~33%, p<0.01; Fig. 2c), despite otherwise normal $Ca_v1.3$ activation properties (Supplementary Table 2). This difference was not observed at P6-8 (p=0.59, Fig. 2d), consistent with sparse synaptic localization of harmonin at this age (Fig. 1g). Ca^{2+} microdomains, which primarily reflect presynaptic Ca^{2+} influx[10], had higher amplitudes in mature *dfcr* than control IHCs (~53%, p=0.02; Fig. 2e, f). Taken together, these results show that harmonin directly inhibits synaptic $Ca_v1.3$ channel density in IHCs, which is disrupted by the *dfcr* mutation.

Cell surface density of ion channels can be regulated by ubiquitination and targeting for proteosomal or lysosomal degradation[11]. Thus, we tested if harmonin enhanced ubiquitination of $Ca_v1.3$ in HEK293T cells. Following immunoprecipitation with $\alpha_1 1.3$ antibodies, western blotting revealed higher levels of ubiquitinated channels cotransfected with harmonin, which was intensified by the proteosomal inhibitor MG132 (Fig. 3a,b). In addition, harmonin altered the distribution of cell-surface $Ca_v1.3$ channels immunofluorescently labeled through an extracellular hemagglutinin epitope. While $Ca_v1.3$ channels alone showed a fairly continuous distribution, harmonin caused $Ca_v1.3$ channels to form large clusters in the plasma membrane (Fig. 3c, Supplementary Fig. 3). The patchier cell-surface distribution of $Ca_v1.3$ channels caused by harmonin was reversed by MG132 (Fig. 3c). Given that MG132 broadly affects the ubiquitin system and may affect both

proteosomal and lysosomal protein pathways, the altered distribution of $Ca_v1.3$ channels caused by harmonin may result from improper trafficking and/or degradation of ubiquitinated channels. Although $Ca_v\beta$ subunits inhibit ubiquitination of Ca_v channels[12,13], the inhibition of $Ca_v1.3$ current density by harmonin did not require $Ca_v\beta$ (Fig. 3d) but was blocked by MG132 (Fig. 3e; MG132 did not affect current density in cells with $Ca_v1.3$ alone, Supplementary Fig. 4). We conclude that harmonin tags $Ca_v1.3$ channels for ubiquitination and alters their functional levels at the cell surface. This may constrain the number of available presynaptic $Ca_v1.3$ channels in IHCs, a parameter that varies between IHC synapses[10] and during development[14]. Together with evidence that harmonin regulates mechanotransduction currents[8,15], our findings reveal harmonin as not simply a scaffold, but an integral component of ion channel complexes and fundamental regulator of electrical and Ca^{2+} signaling in auditory hair cells.

Supplementary Material

Refer to Web version on PubMed Central for supplementary material.

Acknowledgments

This work was supported by the NIH (DC009433, HL087120, DC 10382 (AL); DC008417 (ICJ); DA015040, K12/GM000680 (FDG); Deafness Research Foundation (AL, ICJ); DFG (Center for Molecular Physiology of the Brain, FZT-103), the BMBF (Bernstein Center for Computational Neuroscience Goettingen: 01GQ1005A) to TM; and Alexander von Humboldt fellowship to TP. The authors thank J.Striessnig for $Ca_V1.3$ KO mice; U. Mueller and U. Wolfrum for cDNAs and antibodies; Q. Zheng for harmonin KO tissue; H.Couchoux, A. Inagaki for contributing data; B. Fritzsch, C.Harata, M.Stamnes, R.Piper for advice and discussion; and J. Diamond for comments on the manuscript.

References

1. Platzer J, et al. Cell. 2000; 102:89–97. [PubMed: 10929716]
2. Brandt A, et al. J Neurosci. 2005; 25:11577–11585. [PubMed: 16354915]
3. Calin-Jageman I, Lee A. J Neurochem. 2008; 105:573–583. [PubMed: 18266933]
4. Verpy E, et al. Nat Genet. 2000; 26:51–55. [PubMed: 10973247]
5. Calin-Jageman I, et al. J Neurosci. 2007; 27:1374–1385. [PubMed: 17287512]
6. Reiners J, et al. Invest Ophthalmol Vis Sci. 2003; 44:5006–5015. [PubMed: 14578428]
7. Boeda B, et al. EMBO J. 2002; 21:6689–6699. [PubMed: 12485990]
8. Grillet N, et al. Neuron. 2009; 62:375–387. [PubMed: 19447093]
9. Johnson KR, et al. Hum Mol Genet. 2003; 12:3075–3086. [PubMed: 14519688]
10. Frank T, et al. Proc Natl Acad Sci U S A. 2009
11. Abriel H, Staub O. Physiology (Bethesda). 2005; 20:398–407. [PubMed: 16287989]
12. Waithe D, et al. J. Biol. Chem. 2011; 286:9598–9611. [PubMed: 21233207]
13. Altier C, et al. Nature neuroscience. 2011; 14:173–180. [PubMed: 21186355]
14. Beutner D, Moser T. J Neurosci. 2001; 21:4593–4599. [PubMed: 11425887]
15. Michalski N, et al. Pflugers Arch. 2009; 459:115–130. [PubMed: 19756723]

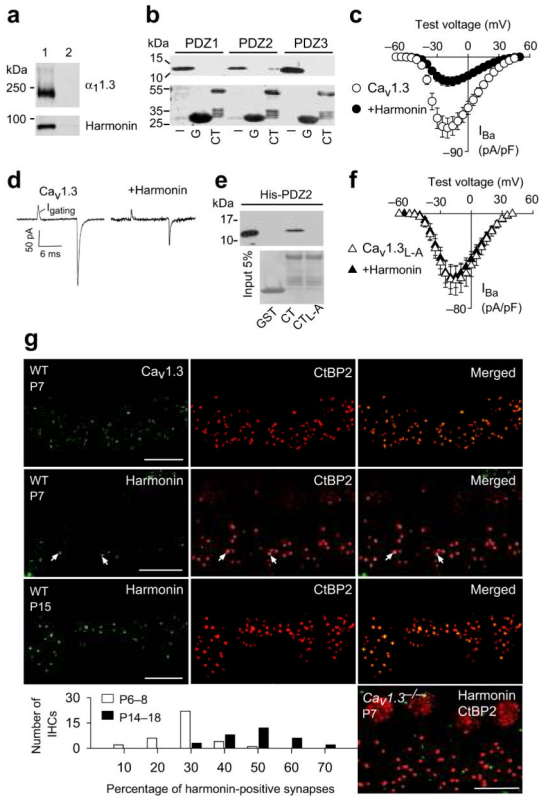

Figure 1.

Harmonin inhibits $Ca_v1.3$ channels and is localized at inner hair cell synapses.

(a) Myc-harmonin coimmunoprecipitates with FLAG-$\alpha_1$1.3 in cotransfected HEK293T cells (lane 1) but not in cells transfected with myc-harmonin alone (lane 2). (b) Western blot (upper panel) from pull-down assay shows GST-1.3CT (CT) but not GST (G) binds his-tagged PDZ2 of harmonin. Input (I) represents ~5% protein His-PDZ protein input. Ponceau staining (lower panel) shows amounts of GST-proteins used. Full length blots are presented in Supplementary Fig.5. (c) Harmonin inhibits $Ca_v1.3$ I_{Ba} density in transfected HEK293T cells. $Ca_v1.3$ alone, n=11; +harmonin, n=11. (d) Representative traces showing gating currents (I_{gating}) of $Ca_v1.3$ ± harmonin measured at the I_{Ba} reversal potential (+60 mV). (e) His-PDZ2 of harmonin binds to $\alpha_1$1.3 CT but not with L-A mutation. Pull-down assay was done as in *b*. (f) No effect of harmonin on I_{Ba} density for $Ca_v1.3$ with L-A mutation ($Ca_v1.3_{L\text{-}A}$). $Ca_v1.3_{L\text{-}A}$ alone, n=8; $Ca_v1.3$+harmonin, n=7. (*g*) Confocal projections of whole mounts of Organ of Corti from wild-type (WT, P7 or P15) or *$Ca_v1.3^{-/-}$* mice (P7) double-labeled for CtBP2 (red) and $Ca_v1.3$ (green) or harmonin (green). Synaptic labeling of CtBP2 appears as spots basal to the nucleus, which is also labeled by these antibodies. Areas of colocalization (arrows) are yellow in the merged images. Scale bars, 10 μm. Graph shows distribution of harmonin-positive synapses in individual IHCs from P6–8 and P14–16 IHCs. In *c* and *f*, error bars represent s.e.m.

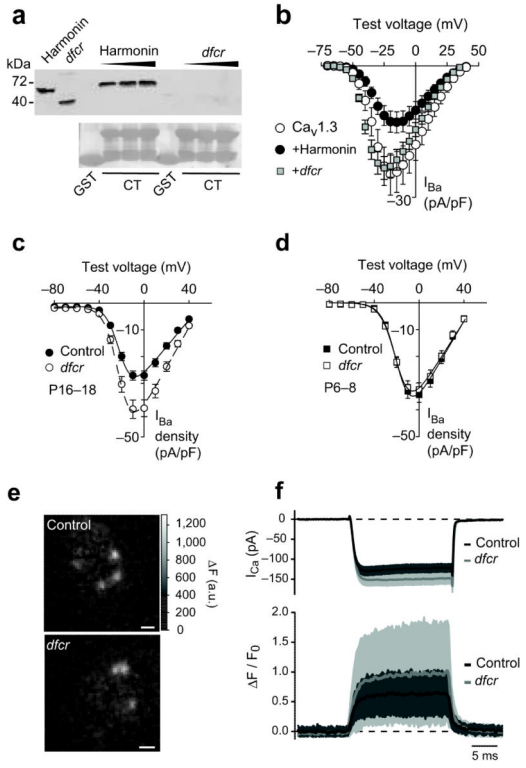

Figure 2.

Dfcr mutation prevents functional interaction of harmonin and $Ca_v1.3$

(a) Pull-down assays with GST or GST-$\alpha_1$1.3 CT and increasing amounts of lysates from HEK293T cells transfected with myc-harmonin or myc-*dfcr* harmonin, as indicated. Left 2 lanes show input (~5%) and Ponceau staining (lower panel) shows GST or GST-$\alpha_1$1.3 CT used in the assay. Full length blots are presented in Supplementary Fig.5. (b) Same protocol as in Fig.1c except in cells transfected with $Ca_v1.3$ alone, n=7, +harmonin, n=9, or +*dfcr*-harmonin, n=8. (c,d) Plots of I_{Ba} density vs. test voltage from whole-cell patch clamp recordings at P16-18 (c) and P6-8 (d) from control (+/−; n=23 in *c*, n=45 in *d*) or *dfcr* (−/−; n=31 in *c*, n=42 in *d*) IHCs. (e,f) Simultaneous whole-cell patch clamp recordings and fluorescent measurement of presynaptic Ca^{2+} microdomains. (e) Representative hotspots of Fluo-5N fluorescence in control (+/+) and *dfcr* (−/−) IHCs during depolarization. Scale bar, 1 μm. (f) *Top*, Whole-cell I_{Ca} recorded in control (black line and dark grey area, n = 14) and *dfcr* (grey line and light grey area, n = 16) IHCs. *Bottom*, Background-subtracted and normalized Fluo-5N fluorescence change ($\Delta F/F_0$, mean±SD) in the center of the Ca^{2+} microdomain (41 domains in 14 control IHCs and 41 domains in 16 *dfcr* IHCs). In *b-d*, error bars represent s.e.m. Protocols for the use of mice were approved by the Institutional Animal Care and Use Committee at U. Iowa and U. Gottingen.

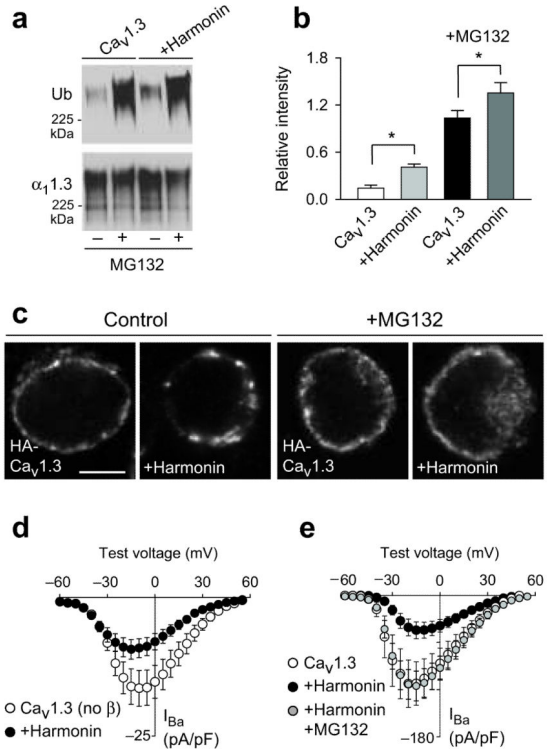

Figure 3.

Harmonin inhibits plasma membrane $Ca_v1.3$ channel density through a ubiquitin-dependent pathway

(a,b) Ubiquitination of $Ca_v1.3$ channels in HEK293T cells transfected with $Ca_v1.3$±harmonin. $Ca_v1.3$ channels were immunoprecipitated with $\alpha_1$1.3 antibodies and western blotting was performed with anti-ubiquitin (Ub, top panel) or $\alpha_1$1.3 antibodies (bottom panel). Cells were maintained with (+) or without (−) MG132 (5 μM, 12 h) prior to lysis. Ubiquitination of $Ca_v1.3$ was quantitated and plotted as relative intensities (b); *, $p<0.05$. Full length blots are presented in Supplementary Fig.5. (c) Confocal micrographs showing immunofluorescence of cell-surface labeled HA-$Ca_v1.3$ channels transfected alone or with harmonin. Pretreatment with MG132 was as in (a). Scale bars, 5 μm. (d,e) I_{Ba} density recorded as in Fig.1c in HEK293T cells cotransfected without $Ca_v\beta$ (d; n=12 for $Ca_v1.3$, n=11 for +harmonin) or with $Ca_v\beta$ (e; n=12 for $Ca_v1.3$ alone, n=14 for +harmonin, n=11 for +harmonin+MG132). In (e), cells were treated with MG132 (5 μM) 1-3 h before recording. In *b*, *d*, *e*, error bars represent s.e.m.